II.G.12 Photoelectrochemical Materials: Theory and Modeling

John Turner (Primary Contact), Wanjian Yin, Su-Huai Wei, Mowafak Al-Jassim, and Yanfa Yan
National Renewable Energy Laboratory
1617 Cole Blvd.
Golden, CO 80401
Phone: (303) 275-4270
E-mail: John.Turner@nrel.gov

DOE Manager
HQ: Eric Miller
Phone: (202) 287-5829
E-mail: Eric.Miller@hq.doe.gov

Project Start Date: 2007
Project End Date: Project continuation and direction determined annually by DOE

Fiscal Year (FY) 2011 Objectives

The main focus of the project is to:

- Understand the performance of current photoelectrochemical (PEC) materials.
- Provide guidance and suggest solution for performance improvement.
- Design and discover new materials.
- Provide theoretical basis for Go/No-Go decisions on PEC activities.

Technical Barriers

This project addresses the following technical barriers from the PEC water-splitting section of the Fuel Cell Technologies Program Multi-Year Research, Development and Demonstration Plan:

(Y) Materials Efficiency
(Z) Materials Durability
(AB) Bulk Materials Synthesis

Technical Targets

This project provides a theoretical understanding of the performance of current PEC materials and provides feedback and guidance for performance improvement.

FY 2011 Accomplishments

- Proposed the general strategies for the rational design of semiconductors to simultaneously meet all of the requirements for high-efficiency, solar-driven PEC water splitting materials.
- Studied the intrinsic and extrinsic doping properties of $BiVO_4$ and proposed good candidates for *p*-type dopants (Sr_{Bi}, Ca_{Bi}, Na_{Bi}, K_{Bi}) and *n*-type dopants (W_V and Mo_V).

Introduction

The electronic band structures of semiconductors are crucial for the performance of semiconductor-based PEC water-splitting. The requirements of those semiconductors include the following tightly coupled material property criteria: appropriate band gap (1.6-2.2 eV), efficient visible light absorption, high carrier mobility, and correct band-edge positions that straddle the water redox potentials. Trail-and-error synthesis approaches have proven ineffective in discovering a viable material, and the band structure engineering for existing materials is necessary [1,2]. So far, most of existing work on band structure engineering is to reduce the band gap without considering other tightly coupled properties described above [2-4]. As a result, the PEC efficiency sometimes became worse when impurities were introduced. It is critical to develop general strategies to address all the requirements simultaneously rather than only reducing band gap.

As an example, anatase TiO_2 is one of the most studied materials owing to its good photocatalytic activity, ease of synthesis, long-term chemical stability, and demonstrated PEC applications. However, its large band gap (~3.2 eV) fails to absorb a significant fraction of visible light, resulting in poor solar-to-hydrogen conversion efficiency. Great efforts have been devoted to chemically engineer TiO_2 to reduce its band gap but with only marginal success. For example, monodoping with impurities such as N or C in TiO_2 has been applied to reduce the band gap of TiO_2. However, the high concentration of these impurities needed for band gap reduction causes serious carrier recombination and produces inferior material quality, making efficient solar-to-hydrogen conversion impossible.

Our previous work demonstrated that donor-acceptor codoping can effectively enhance the PEC properties of ZnO due to the reduction of the recombination centers [5,6]. In the last year, we extended the donor-acceptor codoping concept to engineer the bandgap of TiO_2. We explored how the codoping would affect the other tightly coupled properties. We found that the properties are connected tightly with the concentration of dopants.

$BiVO_4$ has shown particular promise for water photodecomposition with the presence of both a low bandgap (2.4–2.5 eV) and reasonable band-edge alignment

with respect to the water redox potentials [7-9]. For implementation in the real device, both of the good *n*-type and *p*-type doping properties should be required to form Ohmic contacts with contact materials. However, to date, the intrinsic and extrinsic doping properties of $BiVO_4$ haven't been systematically explored.

Approach

We employ density functional theory (DFT) to study the electronic properties of the anatase TiO_2 and $BiVO_4$ and how doping would affect their electronic properties. Generalized gradient approximation (GGA) to DFT and the projected augmented wave basis as implemented in the Vienna *ab initio* simulation package (VASP) [10] are used. The plane-wave cut-off energy of 400 eV was used, and the ion positions were always relaxed until the force on each of them is 0.01 eV/Å or less. For TiO_2, the impurity co-incorporation was modeled using (2×2×1) supercells with a total of 48 atoms which randomly include the impurity pairs. The supercell sizes were allowed to relax. The k-point sampling was 7×7×3 for the conventional cell of anatase TiO_2 and equivalent k points for large supercells. The band offset was calculated by aligning the average potentials of host elements far away from impurities with that in pure bulk cell. The GGA band gap error was corrected using a scissor operator. For $BiVO_4$, the dopants were incorporated into a (2×1×2) supercell with 96 atoms. The k-point sampling was 2×3×3 for the supercell. For defect formation energy and transition energy calculation, the combined schemes of both Γ-point and special k-points were used which could predict the transition energy more precisely [11,12].

For rational band structure engineering of TiO_2, we have proposed four general strategies: (i) utilizing charge balanced donor-acceptor alloying to overcome solubility limit, reduce charged defects, and improve the quality of materials; (ii) using higher 4*d*, 5*d* transition metals substitution on Ti sites to lift up the conduction band; (iii) using C, N with higher 3*p* substitution in O site to raise the valence band and thus reduce the band gap; and (iv) using high concentration of the alloying elements to enhance optical absorption and improve the hole mobility.

Results

We first discuss the energetic favorability of donor-acceptor codoping. The incorporation of a single foreign element can often be limited by the solubility limit in host materials. In the case of high concentration, it may create other detrimental issues such as undesirable charged defects, inferior materials quality, and too high carrier concentration. Our previous work on ZnO showed that the donor-acceptor codoping could enhance doping concentration while keeping good carrier mobility. The charge transfer between the donor and acceptor and the interactions between these two neighbors play key roles. We investigated the interaction behavior of donor and acceptor in TiO_2. Table 1 shows the binding energies of various donor-acceptor pairs considered in our work.

TABLE 1. Binding Energies of Various Donor-Acceptor Pairs

Pairs	E_b(eV)	Pairs	E_b(eV)	Pairs	E_b(eV)	Pairs	E_b(eV)
(Cr,C)	3.02	(Nb,N)	1.97	(Zr,S)	-0.50	(2Ta,C)	1.82
(Mo,C)	3.24	(Ta,N)	1.92	(Hf,S)	-0.56	(2Nb,C)	2.11
(W,C)	2.86	(Ta,P)	0.40	(Zr,Se)	-0.37	(Mo,2N)	4.78
(V,N)	2.25	(Nb,P)	0.58	(Hf,Se)	-0.44	(W,2N)	4.80

Except for the Zr and Hf, the binding energies of donor-acceptor pairs are positive which means that the donor and acceptors favor to combine with each other, thus enhancing the solubility. The reason for negative values for Zr and Hf is that the Zr and Hf are isovalent to Ti and the substitutions don't have large charge transfer between cation and anion dopants.

Taking (Ta, N) as an example, Figure 1 shows that concentration of the incorporated donor and acceptor can affect significantly the electronic properties of TiO_2. Increasing the alloy concentration not only can further reduce the band gap, but can also simultaneously enhance the optical absorption in the long-wavelength regions and reduce the carrier effective mass. The results clearly show that as the concentration increases, the N 2*p* band broadens, the band gap decreases, and the dispersion of the N 2*p* band increases, leading to higher carrier mobility. The GGA calculated band gap reduction increased to 0.70 eV when 12.5% O is replaced by N. Figure 2 shows calculated optical absorption coefficient spectra for (Ta,N) co-incorporated TiO_2 with various concentrations. The results show clearly that as the concentration of (Ta,N) pairs increases, the absorption in the longer-wavelength region is dramatically enhanced. Most previous calculations have only focused in the low-concentration regime. Our results show, however, that there is a strong dependence of the band gap on the alloy concentration. The band-gap reduction predicted at the low-alloy concentration may not be applicable to the high-alloy concentration cases. Therefore, to provide a rational prediction of the band gap and band-edge positions, the calculations should be conducted at both low- and high-alloy concentrations.

Figure 3 shows the calculated band gaps and band-edge alignments in both of the low (Figure 3a) and high (Figure 3b) concentration regime. The results show that the incorporation of Ta, Nb, Zr, and Hf as donors can lead to desirable upshifts of the conduction band minimum (CBM) (marked by red positive values). The incorporation of Cr, Mo, W, and V lead to an unwanted downshift of the CBM. The calculated trends for the valence band maximum (VBM) are also consistent with these atomic trends. The (2Nb,C), (2Ta,C), (Mo,2N), and (W,2N) combinations give both better band gap reduction and band-edge positions. However, the (Mo,2N) and (W,2N) combinations are expected to produce

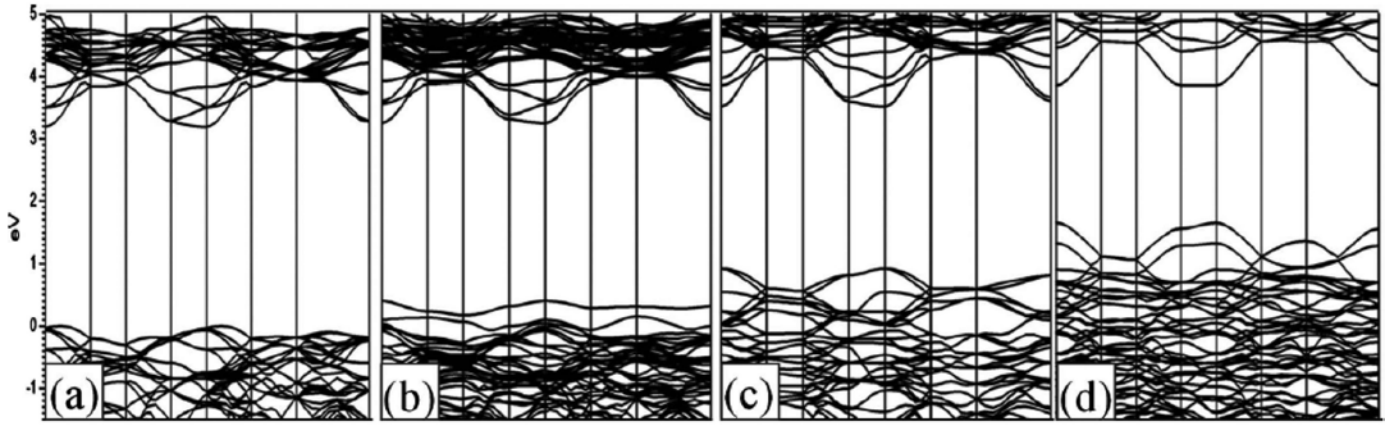

FIGURE 1. The band structures of (a) pure TiO_2, (b) 3.1% (Ta, N) co-incorporated TiO_2 with 3.1% O replaced by N, (c) (Ta, N) co–incorporated TiO_2 with 12.5% O replaced by N, (d) (Ta, N) co–incorporated TiO_2 with 25 % O replaced by N. The CBMs are aligned for guide of eyes as the conduction band structure characters near CBM are nearly unchanged.

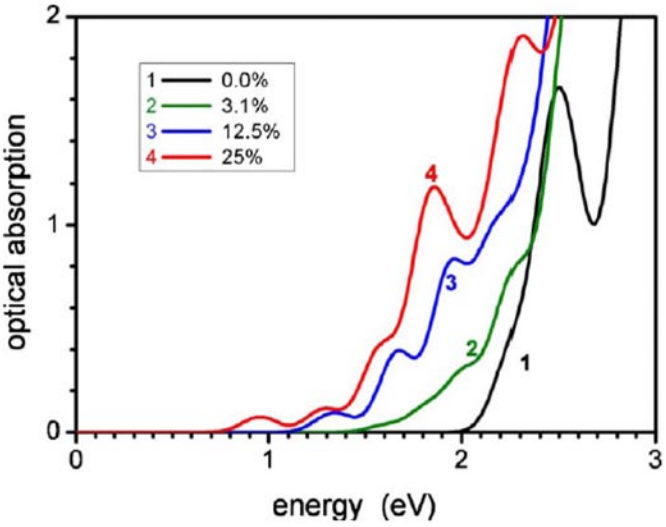

FIGURE 2. Optical absorption spectrum (the part near absorption edge) of pure TiO_2 and (Ta, N) co–incorporated TiO_2 with 3.1%, 12.5%, and 25% of O replaced by N, respectively.

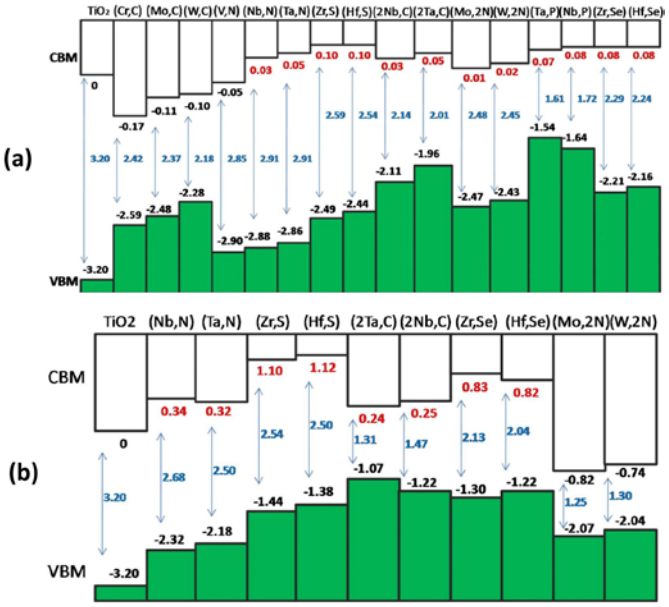

FIGURE 3. Calculated GGA band offset (at Γ point) for TiO_2 and TiO_2 alloyed with various donor-acceptor combinations in the (a) low-concentration regime and (b) high concentration regime. The CBM of pure TiO_2 is set to zero as the reference and the band gap is corrected by scissor operator.

more dispersive defect bands. At high concentration, TiO_2 co-incorporated with (Cr,C), (Mo,C), (W,C), and (V,N) becomes metallic due to too much band broadening of both unoccupied and occupied bands created by the donors and acceptors. The combinations used to give good band gaps in the low-concentration regime such as (2Nb,C), (2Ta,C), (Nb,P), and (Ta,P) now give band gaps that are too narrow due to their high VBM. While (Nb,N) and (Ta,N) combinations give the desirable band gaps estimated to be 2.68 eV and 2.50 eV, respectively, simultaneously with proper band-edge positions. Our results, therefore, suggest strongly that the band-edge positions and band gaps depend critically on the concentration of the incorporated donors and acceptors pairs. As a general guidance, one must consider carefully band gaps and concentration at the same time so that the appropriate donor-acceptor combinations can be chosen.

Simultaneously considering the band gap, band edge and binding energies, we predict that (Ta,N) and (Nb,N) pairs are the optimal donor-acceptor combinations in the high concentration regime, and (Mo,2N) and (W,2N) combinations are good candidates in the low-concentration regime for engineering TiO_2 for PEC water-splitting.

The properties of intrinsic defects in $BiVO_4$ were studied. Our results show that the Fermi level is always

pinned by Bi vacancy and O vacancy. Under O poor conditions, the Fermi level is pinned at ~0.35 eV below CBM and under O rich condition, the Fermi level is pinned at ~0.55 eV above VBM. As a result, without external doping, $BiVO_4$ should only exhibit moderate *n*-type or *p*-type conductivities, which is needed for good PEC absorbers.

We calculated the transition energies and formation energies for group-I, group-II, group-IV elements as dopants. We found that outstanding *p*-type conductivity can be achieved by Br, Ca, Na, or K doping at O-rich growth conditions because these impurities at Bi sites are shallow acceptors and have rather low formation energies. Excellent *n*-type conductivity can be realized by Mo or W doping at O-poor growth conditions, because they are very shallow donors at V sites and have very low formation energies. Figure 4a shows the formation energies of group-II (Zn, Mg, Ca, Sr) elements as p-type doping doping in O-rich conditions. The dashed lines are the curve of the lowest formation energy of the intrinsic defects. All the possible configurations of impurities, such as substitution and interstitials, are considered. It is seen that Ca and Sr exhibit excellent p-type doping properties, not only because their shallow transition energies (around 0.1 eV), but also because their formation energies are lower than that of intrinsic defects.

Figure 4 shows the formation energies of group-VI (Cr, Mo, W) elements doping in O-poor conditions. The Mo and W dopants exhibit good *n*-type properties. The (0/1+) ionization energies of Mo_V is as shallow as 0.04 eV. W_V is even shallower (0.01 eV), but its formation energy is a little higher than Mo_V, making the Fermi level pinning with Bi vacancy and thus the Fermi level is located at ~0.2 eV below CBM. Therefore, Mo and W are good candidates that could lead to excellent n-type conductivity in $BiVO_4$.

The impurities discussed in the above calculation are mostly on cation sites. On the other hand, *p*-type and *n*-type doping of metal oxides may also be realized by introducing impurities to O sites. In this case, C, N, and F are the most considered impurities. Because interstitials of these impurities usually have large formation energies, we will only consider substitutional defects, C_O, N_O, and F_O. However, these conventional dopants are not expected to lead to good p-type or n-type conductivities.

Conclusions and Future Direction

We have proposed general strategies for the rational design of semiconductors to simultaneously meet all of the requirements for a high-efficiency PEC water splitting material. As a case study, we applies our strategies for engineering anatase TiO_2. Previous attempts to modify known semiconductors often focused on a particular individual criterion. Our theoretical results show that with appropriate donor-acceptor coincorporation alloys with anatase TiO_2 hold great potential to satisfy all of the criteria for a viable PEC device. We predict that (Mo,2N) and (W, 2N) are the best donor-acceptor combinations in the low-alloy concentration regime whereas (Nb, N) and (Ta, N) are the best choice of donor-acceptor pairs in the high-alloy concentration regime.

Without external dopants, $BiVO_4$ exhibits moderate *p*-type in O-rich condition and moderate n-type in O-poor condition, which is just needed for good PEC absorber. On the other hand, for external dopants, Sr, Ca, Na, and K are proposed to be good p-type dopants and the Mo and W are proposed to be good *n*-type dopants for $BiVO_4$, which is needed for forming Ohmic contacts between absorber and

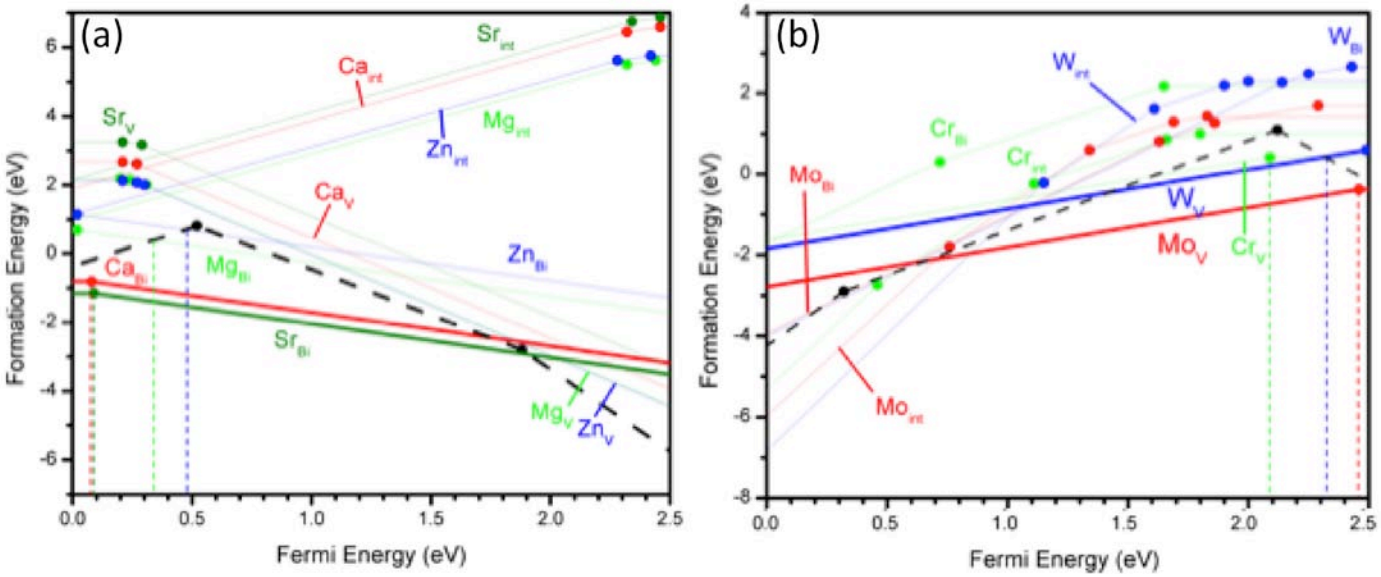

FIGURE 4. Calculated formation energies of (a) group-II (Zn, Mg, Ca, Sr) dopants in O-rich conditions and (b) group-VI (Cr, Mo, W) dopants in O-poor conditions.

contacts. C, N and F are found not to be good candidates for p-type or n-type doping of BVO_4.

Future direction includes the following:

- Apply the design strategies to engineer other metal oxides, such as Fe_2O_3.
- Understand the electronic properties of other metal oxides.
- Design new metal oxides for PEC applications.

FY 2011 Publications/Presentations

1. W.-J. Yin, H.W. Tang, S.-H. Wei, J. Turner, M.M. Al-Jassim, Yanfa Yan, "Band structure engineering of semiconductors for enhanced PEC water splitting" *Phys. Rev. B **82**, 045106 (2010)*.

2. W.-J. Yin, S.-H. Wei, M. M. Mowafak, J. Turner, and Yanfa Yan, "Doping properties of monoclinic BiVO4 studied by the first-principle density-functional theory" *Phys. Rev. B **83**, 155102 (2010)*.

3. L. Chen, S. Shet, H.W. Tang, H.L. Wang, T. Deutsch, Yanfa Yan, J. Turner, M. Al-Jassim, "Electrochemical deposition of copper oxide nanowires for photoelectrochemical applications," J. Mater. Chem., 20, 6962 (2010).

4. L. Chen, S. Shet, H. Tang, K.-S. Ahn, H. Wang, Yanfa Yan, J. Turner, and M. Al-Jassim, "Amorphous copper tungsten oxide with tunable band gaps, " J. Appl. Phys. 108, 043502 (2010).

5. S. Shet, K.S. Ahn, T. Deutsch, H. Wang, R. Nuggehalli, Yanfa Yan, J. Turner, M. Al-Jassim, "Influence of gas ambient on the synthesis of co-doped ZnO:(Al,N) films for photoelectrochemical water splitting," J. Power Source 195, 5801-5805 (2010).

6. S. Shet, K.-S. Ahn, H. Wang, R. Nuggehalli, Y. Yan, J. Turner, and M. Al-Jassim, "Effect of substrate temperature on the photoelectrochemical responses of Ga and N co-doped ZnO films," J. Mater. Sci. 45, 5218-5222 (2010).

7. M. Huda, A. Walsh, Yanfa Yan, S.-H. Wei, and M.M. Al-Jassim, "Electronic, structural, and magnetic effects of 3d transition metals in hematite," J. App. Phys. 107, 123712 (2010).

8. W.-J. Yin, S. Chen, J.-H. Yang, X.-G. Gong, Yanfa Yan, S.-H. Wei, "Effective band gap narrowing of anatase TiO_2 by strain along a soft crystal direction," Appl. Phys. Lett. 96, 221901 (2010).

9. S. Shet, K.S. Ahn. T. Deutsch, H.L. Wang, N. Ravindra, Yanfa Yan, J. Tuerner, M. Al-Jassim, "Synthesis and characterization of band gap reduced ZnO:N and ZnO:(Al, N) thin films for photoelectrochemical water splitting," J. Mater. Res. 25, 45 (2010).

References

1. X. Chen and S. S. Mao, *Chem. Rev.* **107**, 2891 (2007).

2. R. Asahi, T. Morikawa, T. Ohwaki, K. Aoki, and Y. Taga, *Science* **293**, 269 (2001).

3. K. Nishijima, B. Ohtani, X. Yan, T. Kamai. T. Chiyoya, T. Tsubota, N. Murakami, and T. Ohno, *Chem. Phys.* **339**, 64 (2007).

4. H. Irie, Y. Watanabe, and K. Hashimoto, *Chem. Lett.* **32**, 772 (2003).

5. K.-S. Ahn, Y. Yan. S. Shet, T. Deutsch, J. Turner, and M. Al-Jassim, *Appl. Phys. Lett.* **91,** 231909 (2007).

6. S. Shet, K.-S. Ahn, Y. Yan, T. Deutsch, K. M. Chrustowski, J. Turner, M. Al-Jassim, N. Ravindra, J. App. Phys. **103**, 073504 (2007).

7. A. Walsh, Y. Yan, M. N. Huda, M. M. Al-Jassim, and S.-H. Wei, *Chem. Mater.* **21**, 547 (2009).

8. H. Luo, A. H. Mueller, T. M. McCleskey, A. K. Burrel, E. Bauer, and Q. X. Jia, *J. Phys. Chem. C* **112**, 6099 (2008).

9. K. Sayama, A. Nomura, T. Arai, T. Sugita, R. Abe, M. Yanagida, T. Oi, Y. Iwasaki, Y. Abe, and H. Sigihara, *J. Phys. Chem. B* **110**, 11352 (2006).

10. G. Kresse and J. Furthmüller, *Comput. Mater. Sci.* **6**, 15 (1996).

11. S.-H. Wei, *Comp. Mater. Sci.* **30**, 337 (2004).

12. Y. Yan and S.-H. Wei, *phys. stat. sol. (b)* **4**, 641 (2008).